Journal of Artificial Organs (2019) 22:276–285
https://doi.org/10.1007/s10047-019-01117-3

ORIGINAL ARTICLE

Artificial Heart (Basic)

Mathematical evaluation of cardiac beat synchronization control used for a rotary blood pump

Daisuke Ogawa[1] · Shinji Kobayashi[1] · Kenji Yamazaki[2] · Tadashi Motomura[3] · Takashi Nishimura[4] · Junichi Shimamura[5] · Tomonori Tsukiya[5] · Toshihide Mizuno[5] · Yoshiaki Takewa[5] · Eisuke Tatsumi[5]

Received: 27 January 2019 / Accepted: 8 July 2019 / Published online: 20 July 2019
© The Japanese Society for Artificial Organs 2019

Abstract

We studied a control method of rotary blood pumps (RBPs), which is called as the cardiac beat synchronization (CBS) system. Usually, RBPs operate at constant target rotational speed, meanwhile, the CBS system modulates target speed synchronizing with cardiac beat. We built a computer simulation method to evaluate the CBS system. This simulator acquires a mathematical model of a circulatory system including a RBP and can provide us the theoretical hemodynamics when our control method is applied. We compared theoretical results with experimental ones with the model focusing on both pulsatility and aortic valve (AV) opening interval enhanced by the CBS system. Our simulator could reproduce behavior of the circulatory system whether the RBP is connected or not. Comparison among no RBP, constant assist, systolic assist, and diastolic assist modes indicated that pulsatility is enhanced with systolic assist theoretically. While systolic assist decreased AV opening interval, diastolic assist made it longer than the ones in other control strategies.

Keywords Rotary blood pump · Synchronization with cardiac beat · Pulsatility · Simulation

Introduction

Left ventricular assist devices (LVADs) based on rotary blood pumps (RBPs) are widely used for patients suffering from cardiac diseases. Quality of life (QOL) has been improved by the progress in development of RBPs.

We had studied a control method of RBPs, which is called as a cardiac beat synchronization (CBS) system. Usually, RBPs operate at constant target rotational speed, meanwhile, the CBS system modulates target speed synchronizing with cardiac beat. We demonstrated that the method enables unloading of the ventricle, prolonging on aortic valve (AV) opening interval, mimicking off test, and so on [1–5]. Pirbodaghi has also reported that modulating rotational speed of a RBP enhances pulsatility [6].

These results are mostly from experimental setups like animal tests. Meanwhile, an actual circulation is a dynamic time-variant system in nature, thus, it is difficult to evaluate all of combinations of parameters, such as vascular impedance, cardiac function, and control configurations of RBPs. Not only experimental results but also theoretical mechanisms should be studied to clarify changes in hemodynamics introduced by the control strategy. We can validate results from actual tests by comparing with theoretical ones in various conditions. Also, computer simulation can highlight small and obscure changes, such as AV opening.

For these issues, we built a computer simulation method to evaluate the CBS system. This simulator acquires a mathematical model of a circulatory system including a RBP and can provides us the theoretical hemodynamics when our control method is applied. Prior researches revealed an interaction between RBPs and a circulatory system with simulation

✉ Daisuke Ogawa
d-ogawa@evaheart.co.jp

1 Sun Medical Technology Research Corp., 2990 Shiga, Suwa-city, Nagano 392-0012, Japan

2 Hokkaido Cardiovascular Hospital, 13 Chome-1-30 Minami 27 Jonishi, Chuo Ward, Sapporo, Hokkaido, Japan

3 Evaheart Inc., 6655 Travis ST, Suite 590, Houston, TX, USA

4 Department of Cardiac Surgery, Tokyo Metropolitan Geriatric Hospital, 35-2 Sakaecho, Itabashi, Tokyo, Japan

5 Department of Artificial Organs, National Cerebral and Cardiovascular Center Research Institute, 5-7-1 Fujishiro-dai, Suita, Osaka, Japan

study; however, operation of RBPs was simply assumed as a constant rotational speed mode or non-synchronized control mode in many cases [7–12]. Vandenberghe [13] and Bozkurt [14] investigated sinusoidal modulation of the rotational speed, but the waveform is different from our implementation. Htet reported co-pulse assist with an axial pump [15], but the counter-pulse mode is another important option.

In this paper, we describe mathematical models derived from circuit models for left heart system including the RBP. We compared theoretical results with experimental ones focusing on both pulsatility and AV opening interval enhanced by CBS system.

Materials and methods

Modeling circulatory system with/without RBP

A circulatory system, which consists of the left ventricle (LV), left atrium, aorta, and RBP, is represented in analogy with an electrical circuit model. Figure 1 shows models, which include and exclude the RBP, respectively. See Table 1 for acronyms used in this paper.

Parameters for vascular resistance, inertia, and compliance were defined as constant values. Windkessel model with 2 elements was used for aortic impedance. Ventricular function was simulated with a time-variant elastance model. The RBP was modeled as a constant power supply.L_p was determined with the trial and error manner referring to animal experimental results. LAP was a constant value, but atrial contraction is added at the end diastole. The contraction was simulated with a sinusoid with an amplitude of + 7 mmHg and a half-cycle period of 0.16 s [7, 8, 16].

Table 1 Abbreviations and acronyms

Acronyms	Component	Abbrev./Value
$p_V(t)$	Left ventricular pressure	LVP
$p_A(t)$	Aortic pressure	AoP
$p_{LA}(t)$	Left atrial pressure	LAP
$p_{BP}(t, i_R(t))$	Blood pump pressure	BP
$V(t)$	Left ventricular volume	LVV
V_0	Left ventricular dead volume	–
$i_A(t)$	Aortic flow	AoF
$i_R(t)$	Pump flow	PF
$i_A(t) + i_R(t)$	Total flow	TF
$E(t, V(t))$	Ventricular elastance	–
$N(t)$	Rotational speed	N
R	Vascular resistance	1.0–1.4
C	Arterial compliance	0.8
r	Aortic resistance	0.05
L_A	Aortic inertance	0.001
L_P	Pump inertance	0.2
R_{MV}	Mitral valve resistance	0.005
AV	Aortic valve	–
MV	Mitral valve	–

Unit: resistance—mmHg s/mL, compliance—mL/mmHg, inertance—mmHg·s/mL

Simulation with differential equation solver

Basic differential equations are derived from the model in Fig. 1. A cardiac cycle consists of isovolumic contraction

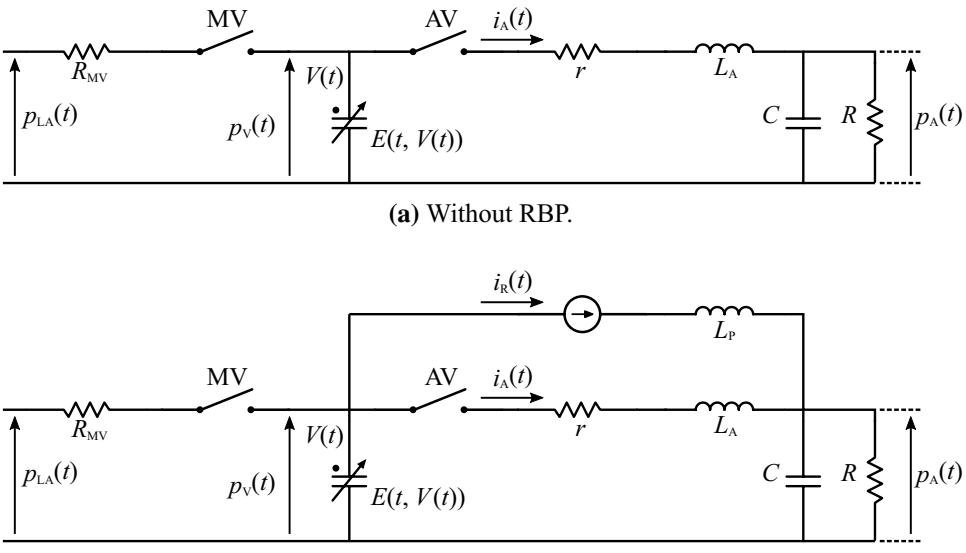

(a) Without RBP.

(b) With RBP.

Fig. 1 Circuit models circulatory systems

phase (ICP), ejection phase (EP), isovolumic relaxation phase (IRP), and filling phase (FP). We can obtain non-homogeneous simultaneous ordinary differential equations (SODEs) for each phase of cardiac cycle of the form (Eq. 1). We can compute numerical solutions with an ordinary differential equation solver, such as R Ver. 3.5.0.

$$\frac{\mathrm{d}}{\mathrm{d}t}x(t) = \mathrm{A}(t)x(t) + b(t) \tag{1}$$

We prepared 8 sets of SODEs for each phase with or without assistance of the RBP (refer to "Appendix"). Simulation of each phase is finished when condition (Eq. 2) is satisfied. The last values in the previous phase are used as initial values for the next phase.

$$\begin{aligned} &\text{ICP: } p_V(t) > p_A(t) \\ &\text{EP: } \ p_V(t) < p_A(t) \\ &\text{IRP: } p_V(t) < p_{LA}(t) \\ &\text{FP: } \ t = t_{\text{end}} \end{aligned} \tag{2}$$

Modeling RBP

In this paper, we simulate the pressure and flow performance of the RBP (P–Q curve) with a polynomial model (Eq. 3).

$$\begin{aligned} p_{BP}\left(t, i_R(t)\right) = &\left\{ \sum_{k=1}^{3} \left(a_k N(t) + b_k\right) {i_R}^k(t) \right\} \\ &+ \left\{ a_0 N^2(t) + b_0 N(t) + c_0 \right\} \end{aligned} \tag{3}$$

Parameters are identified with the measured P–Q curve of EVAHEART® (Sun Medical Tech. Res. Corp.) using the least squares method.

$$\begin{cases} a_k = \left[-2.37 \times 10^{-4},\ 5.55 \times 10^{-3},\ -3.09 \times 10^{-2},\ 8.82 \times 10^{-4} \right] \\ b_k = \left[4.86 \times 10^{-2},\ -1.36 \times 10^{-2},\ 4.48 \times 10^{-1} \right] \\ c_k = \left[-4.04 \times 10^{1} \right] \end{cases} \tag{4}$$

Modeling viscoelasticity of left ventricle

Viscoelasticity of a LV is represented with an elastance curve. We employed a model proposed by Zhong [17], which consists of $E(t, V(t)) = E_a(t) + E_p(V(t))$, where E_a(t) is the active elastance representing the contraction of LV, and $E_p(V(t))$ is the passive elastance representing the ventricular pressure response to ventricular volume change (the so-called Starling's law), respectively. In this study, we used 3 sets of cardiac conditions, middle/upper/lower cardiac function (MCF/UCF/LCF) based on the literature [17].

Analysis

Waveforms obtained from the simulator were evaluated with their averaged/peak-to-peak values. Suffix mean and peak refer to mean and peak-to-peak values in the cardiac cycle, respectively. Pulsatility index (PI) [18] and assist ratio (AR) were calculated with (Eq. 5) and (Eq. 6), respectively. Time resolution was set to 2 ms. Rotational speed N (rpm) was set from 1000 to 2200 rpm per 50 rpm.

$$\mathrm{PI} = \frac{\max\left\{i_R(t)\right\} - \min\left\{i_R(t)\right\}}{\mathrm{mean}\left\{i_R(t)\right\}} \times 10 \tag{5}$$

$$\mathrm{AR} = \frac{\mathrm{mean}\left\{i_R(t)\right\}}{\mathrm{mean}\left\{i_R(t)\right\} + \mathrm{mean}\left\{i_A(t)\right\}} \times 100 \tag{6}$$

In the systolic assist mode, rotational speed was set to $N + N_d$ in systole and $N - N_d$ in diastole, where N_d is difference from original rotational speed in systole and diastole. In diastolic assist mode, rotational speed was set to $N - N_d$ and $N + N_d$ in systole and diastole, respectively. In each case, the waveform becomes square wave whose duty ratio is equal to systolic and diastolic ratios.

Results

Figure 2 shows the simulated waveforms of pressure, volume, flow rate, and miscellaneous data in MCF condition. In these figures, systemic resistance and left atrial pressure increased slightly in each cardiac cycle to obtain end systolic and diastolic pressure–volume relationships (ESPVR and EDPVR, respectively).

Figure 3 shows averaged and peak-to-peak values of total flow, pump flow, aortic flow, and aortic pressure in the case of no RBP/constant assist/systolic assist/diastolic assist, respectively. PI is shown in Fig. 4. N_d was set to 400 rpm in systolic and diastolic assist modes.

$\mathrm{TF_{peak}}$ and $\mathrm{PF_{peak}}$ were enhanced with systolic assist comparing with constant and diastolic assist modes. Pulse pressure, represented by $\mathrm{AoP_{peak}}$, became larger with systolic assist. $\mathrm{AoF_{peak}}$ did not change largely in each assist mode. $\mathrm{TF_{peak}}$ and $\mathrm{AoF_{peak}}$ decreased along with the increase in assist ratio, meanwhile, $\mathrm{PF_{peak}}$ did not change largely by the ratio. In contrast, pulse pressure increased by the ratio. PI also showed that systolic assist promotes pulsatility compared to constant assist, while diastolic assist decreased the index.

Figure 5 shows AV opening interval per assist ratio. In this simulation, aortic valve is opened only in EP passively, thus, the interval is equal to the duration of EP.

Connecting the RBP made AV opening interval shorter compared to the no RBP condition. While systolic assist decreased AV opening interval, diastolic assist made it longer. The interval was obviously prolonged in MCF and UCF conditions, while it was not so clear in LCF condition. There was little difference in the interval when assist ratio was almost close to 100% in each cardiac function.

Fig. 2 Simulated time-series waveforms and *P*–*V* loops

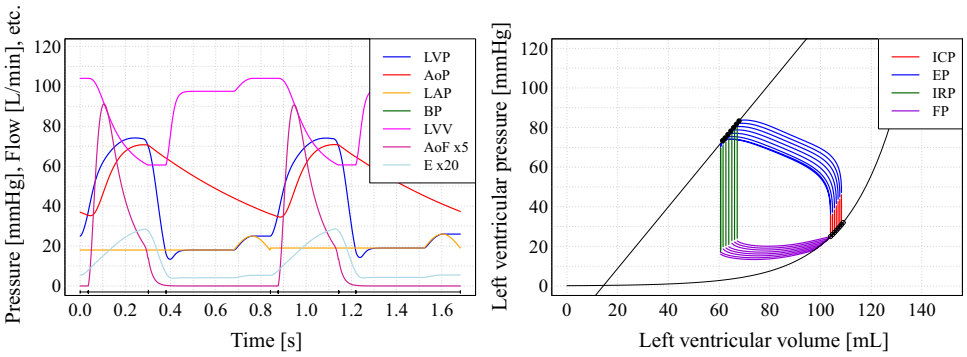

(a) No RBP.

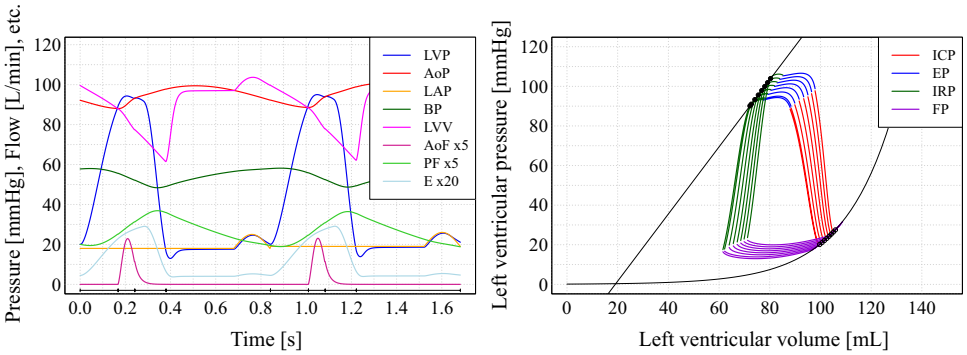

(b) Constant assist ($N = 1600$ rpm).

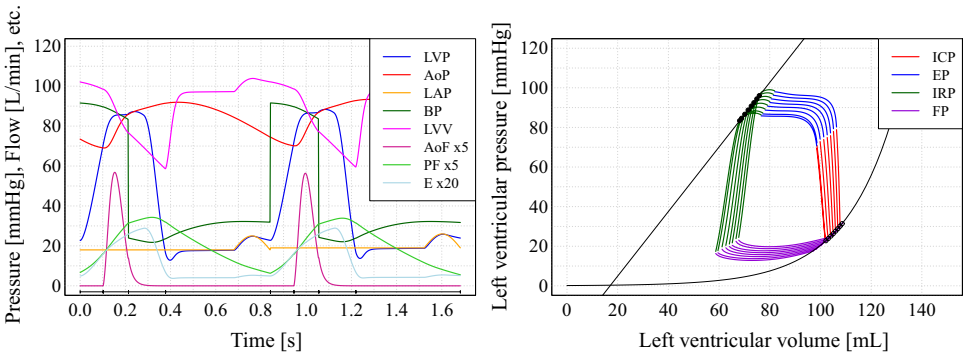

(c) Systolic assist ($N = 1600$ rpm, $N_d = 400$ rpm).

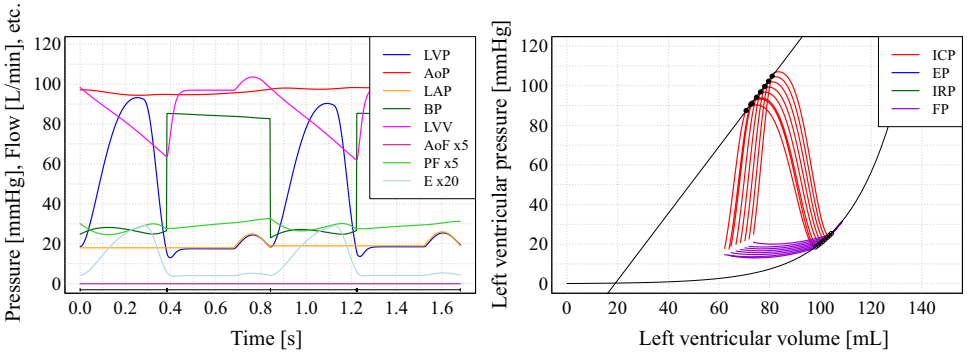

(d) Diastolic assist ($N = 1600$ rpm, $N_d = 400$ rpm).

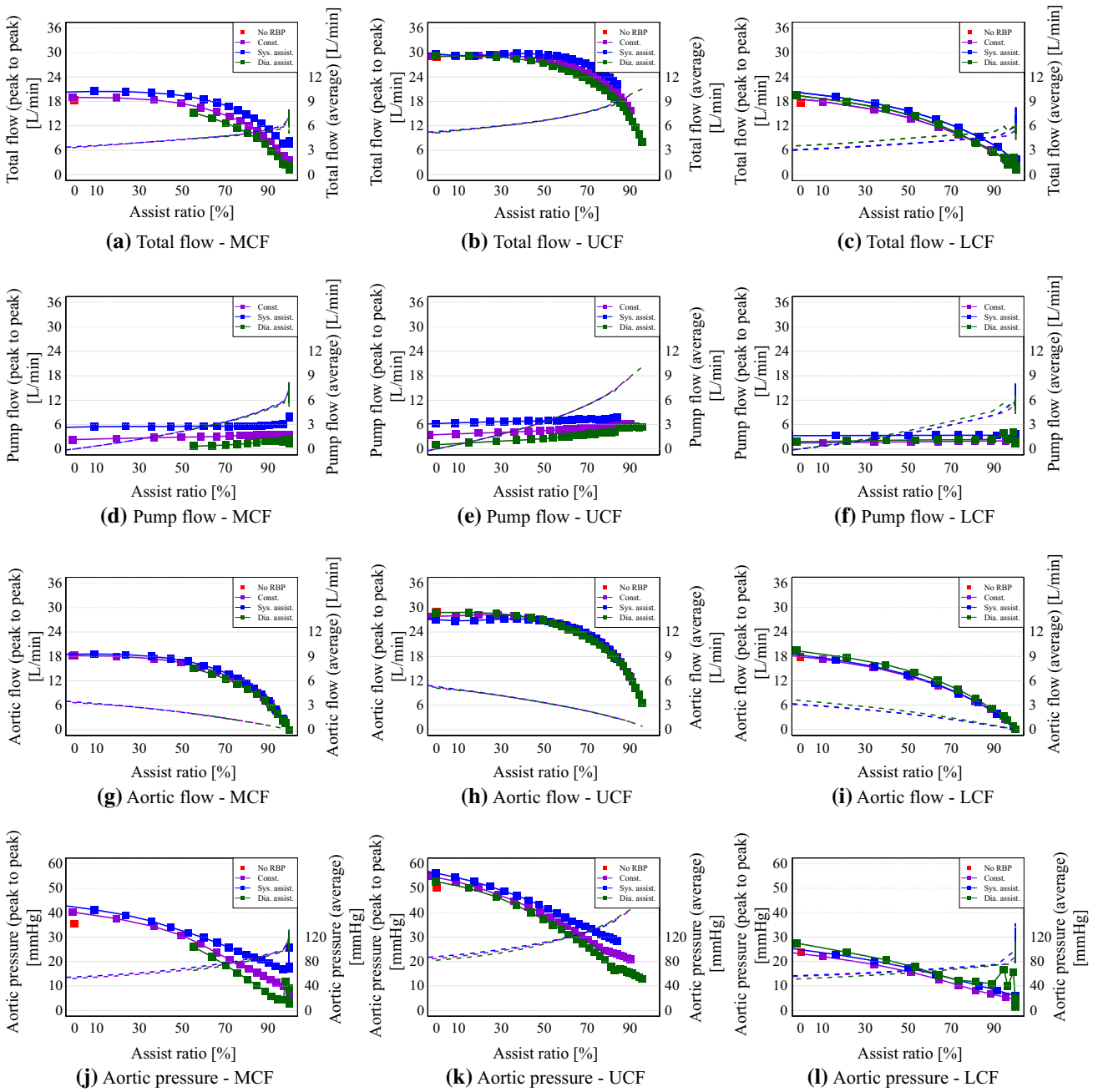

Fig. 3 Total flow, pump flow, aortic flow, and aortic pressure in no RBP/constant assist/systolic assist/diastolic assist per assist ratio (solid line: peak to peak, dashed line: average)

Discussion

Evaluation of proposed simulator

Simulated results with no RBP in Fig. 2 could imitate traditional time-series data and *P*–*V* loop [16, 19]. Besides, hemodynamics in the circulatory system with the RBP is different from the conventional one, which does not include the RBP. For example, both isovolumic contraction and relaxation phases are not isovolumic anymore, since the RBP drains blood from the ventricle. LVV in ICP and IRP are not constant but decreases. In addition, reduced AoP_{peak}, increased AoP_{mean}, and suppressed AoF when rotational speed is higher are common findings shown in clinical cases, animal experiments, and mock studies [1, 20, 21, 22]. In spite of that, our simulator could reproduce such behaviors of the circulatory system even if the RBP is connected.

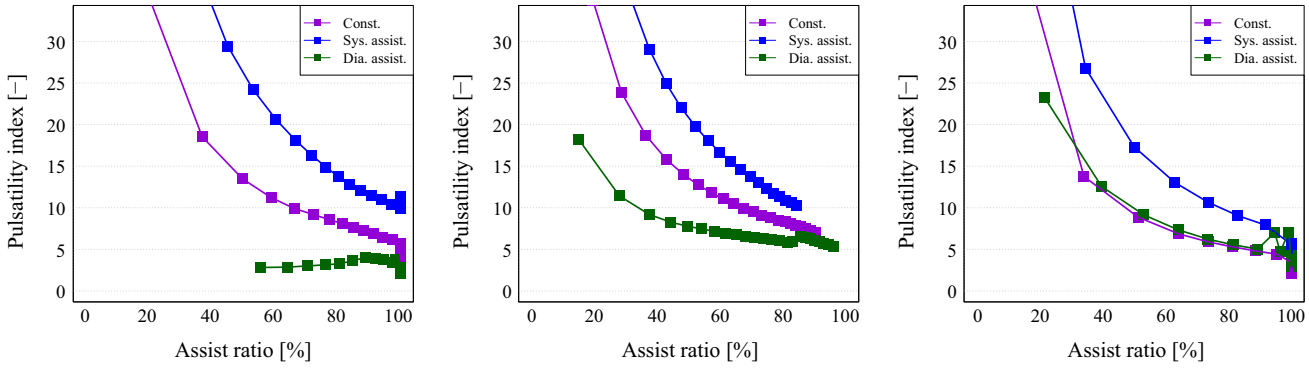

Fig. 4 Pulsatility index in constant assist/systolic assist/diastolic assist per assist ratio

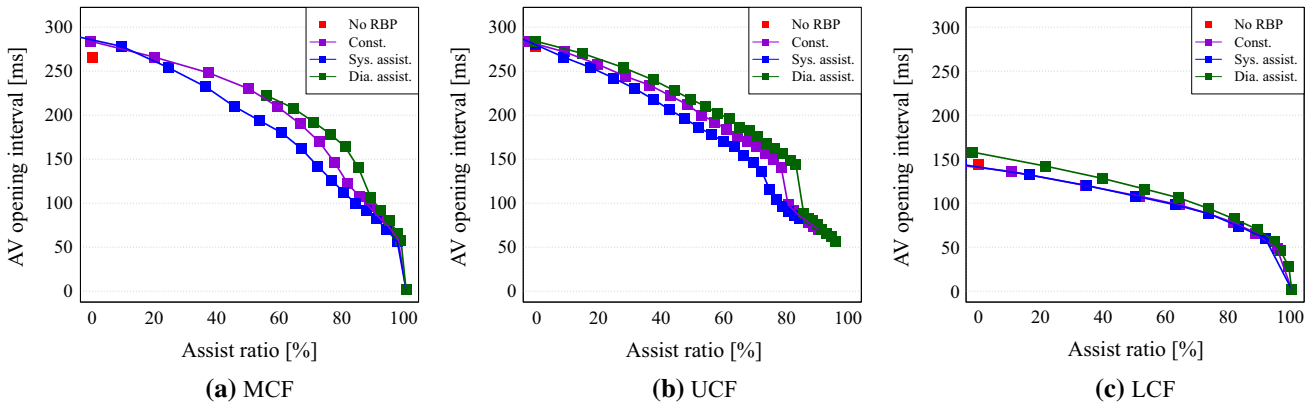

Fig. 5 Aortic valve opening interval in no RBP/constant assist/systolic assist/diastolic assist

Benefits for pulsatility

RBPs generates only constant flow by itself; however, changes in preload or afterload of the RBP caused by contraction of the left ventricle results in an output from the RBP pulsatile. Amplitude of the pulse is mainly determined by the static characteristics of the RBP. Generally, the flatter *P*–*Q* curve generates more pulsatility [18].

Although the concept is clear, there is an interaction between the RBP and the circulatory system, since the RBP changes LVP (preload) by reducing LVV, and AoP (afterload) by outputting flow to aorta, respectively. However, an illustrative explanation with LVP, AoP, and *P*–*Q* curve is informative, but it is not sufficient enough for quantitative evaluation of pulsatility. The relationship becomes more complex when the rotational speed is dynamically changed with CBS control. We employed mathematical simulation to evaluate pulsatility quantitatively.

As shown in Figs. 3 and 4, pulse pressure and PI, which are indices for pulsatility, were increased by systolic assist and decreased by diastolic assist in UCF and NCF conditions. In LCF condition, pulsatility in diastolic assist was a little larger than the one in constant assist.

RBPs boost pump flow when the pressure difference (AoP − LVP) is decreased as shown in *P*–*Q* curves. As pressure swings, the peak-to-peak value of the pump flow becomes larger. The RBP operating at constant rotational speed cannot produce any pulsatility without any change in pressure difference. In contrast, changing rotational speed within the cardiac cycle can alter peak-to-peak value by itself.

In the LCF condition, pulsatility derived from change in rotational speed was superior to the one based on static characteristics. In UCF and NCF conditions, systolic assist emphasized peak values by increasing pressure and flow at systolic phase and decreasing them at diastolic phase. As discussed above, both mechanisms, which are from *P*–*Q* curve and rotational speed modulation, should be taken into account in practical use.

Animal studies showed that systolic assist enhanced pulse pressure [3, 4], pulsatility of carotid artery, and aortic flow

[5]. Our results could indicate enhancement of pulsatility with systolic assist theoretically.

It is known that RBP with a flat *P*–*Q* curve can output pulsatile flow even if pulsatility of LV is relatively small. EVAHEART blood pump can provide more pulsatility due to the flatter *P*–*Q* curve compared with other RBPs [23]. The CBS system can additionally enhance pulsatility with systolic assist.

Imamura [24] reported that pulsatile VADs improve reverse remodeling of the left ventricle with a wider pulse pressure. He also suggested that preserving pulsatility during RBP assist will contribute to a better recovery rate. Systolic assist will possibly promote reverse remodeling with enhanced pulsatility.

Benefits for aortic valve opening

Aortic insufficiency (AI) is sometimes found in the patients with RBPs [25, 26]. Figure 5 showed that AV opening interval was shortened by connecting the RBP. The interval decreases as assist ratio increased by changing the rotational speed.

It is inevitable that by connecting RBP, AoP increased, since BP = AoP − LVP. Additionally, LVP is decreased by RBP with more drainage from LV in systole. Decreased $E_p(V(t))$ due to less volume causes lower dP/dt (slope of LVP on ICP) through Starling's law. In systolic assist, both increased AoP and decreased LVP work together to delay the opening point of AV, where AoP < LVP, and to advance the closing point of AV, where LVP < AoP. In contrast, diastolic assist enhanced the AV opening interval with opposite mechanism.

The main factors for AV opening, such as AoP, LVP, and BP, are all interactive with each other. In Fig. 5, only small differences were found among constant/systolic/diastolic assist when the assist ratio is more than 80%. In the LCF condition, the interval was almost equal in constant and systolic assist mode. In these cases, AoP_{mean} is kept high with a higher pump pressure, while the peak of LVP is lower as pulsatility is reduced. Then, it becomes harder that peak of LVP exceeds AoP in systole. We should note that effect of the control strategy is limited in some cases based on cardiac function and circulatory condition.

Moazami illustrated that the co-pulse mode decreases AV opening interval due to increased arterial pressure during systole [27]. Figure 3 showed that AoP_{peak} increased by systolic assist, while the mean value was not largely modified; in other words, systolic assist increases the aortic pressure in systole than the one in constant assist. Our simulation proved this indication for decreased AV opening theoretically.

Imamura [24] reported that EVAHEART pump can reduce AI. There are several factors that leads to AI, but, a small opening of the valve causes histological changes in AV [28]. Our simulation revealed that diastolic assist can additionally enhance AV opening interval, which has been already improved in constant assist mode with a flatter *P*–*Q* curve. A longer AV opening interval will prevent AV from coaptation.

Tolpen [29] assessed AV opening with a mock circulation and a high-speed camera. The results indicated that a lower rotational speed increased the interval in each cardiac function. It is consistent with our results, but they did not include changes in the rotational speed within a cardiac cycle.

Comparison with simulation studies

Vandenberghe [13] had evaluated their control method for a RBP with simulation; however, they applied sinusoidal modulation to the rotational speed. The duty cycle of a sine wave is 50%, meanwhile, the ratio between systole and diastole is not always 50% but varies from approximately 30 to 60% according to the heart rate [30]. As our CBS controller is capable of adjusting systolic and diastole intervals independently, we can increase or decrease rotational speed within systole and diastole. It also can alter rotational speed not gradually but in a step shape, thus, ideal systole and diastole assist is achieved.

Ising [31] considered the ratio by introducing pulse width, however, the waveform was modified to make the averaged pump flow in each condition become almost equal. In contrast, we did not adjust averaged flow but compared each condition with assist ratio to compare pulsatility and AV opening interval among constant, systolic, and diastolic assist mode, while the effect from assistance of the RBP was almost equal.

Bozkurt reported a simulation study for varying rotational speed within the cardiac cycle [14]. The modulated waveform in the study seems a bit complex, since they tried to regulate total flow in each condition. They insist that the left ventricular volume at end diastole (LVVED) is reduced with the counter-pulse mode. In our simulation, decrease in LVVED was not so obvious in the diastolic assist mode. Their model is for whole circulation, thus, augmented total flow increases LAP and vice versa.

Comparison with in vitro/vivo studies

Bozkurt also reported a method to obtain more pulsatility by keeping pump flow constant [32]. It is remarkable that their results showed that rotational speed was a bit higher in systole, and then, the peak-to-peak values of aortic pressure and pump flow were enhanced when the feedback control was

applied. Our results also showed pulsatility is augmented with systolic assist.

Ising evaluated co-pulse, counter-pulse, and asynchronized modulation of the rotational speed in a mock circulation and bovine model with ischemic heart failure [33]. Their results also revealed co-pulsation increased pulse pressure and counter-pulsation slightly decreased it. Since their mock system and animal model simulated heart failure physiology, their results should be compared to our LCF condition, where it is the worst case among our 3 levels. In our LCF simulation, PI in diastolic assist was almost equal to one in constant assist.

Their experiments include some combinations of configurations, such as rotational speed, modulation amplitude, and frequencies. Our results also include 3 levels of cardiac function and a more detailed resolution of parameters, taking advantage of the computer simulation.

Limitations

Our current RBP model is not a dynamic but a static model. It is commonly seen that the rotational speed of the RBP is passively fluctuated by cardiac contraction [2]. It is possible to simulate that by swinging rotational speed along the cardiac cycle if needed. In this study, we added no modulation to rotational speed in constant assist mode to make the difference among each control mode clear.

Conclusion

Our mathematical model for CBS system could clarify the contribution of the control strategy to pulsatility and AV opening. The simulation demonstrated that systolic assist enhances pulsatility in various cardiac conditions. Diastolic assist will reduce AI by extending AV opening interval when full bypass is avoided.

Compliance with ethical standards

Conflict of interest D. Ogawa and S. Kobayashi are employed by Sun medical Technology Research Corp. K. Yamazaki serves as a consultant to Sun medical Technology Research Corp. T. Motomura is employed by Evaheart, Inc. Other authors declare that there is no conflict of interest.

Appendix

Parameters of SODEs for circulatory system without rotary blood pump

Isovolumic contraction/relaxation phase

Equations are solved with initial conditions.

Ejection phase

$$x(t)=\begin{bmatrix} v(t) \\ i_A(t) \\ p_A(t) \end{bmatrix},\quad b(t)=\begin{bmatrix} 0 \\ 0 \\ 0 \end{bmatrix},\quad A(t)=\begin{bmatrix} 0 & -1 & 0 \\ \frac{E(t,V(t))}{L_A} & -\frac{r}{L_A} & -\frac{1}{L_A} \\ 0 & \frac{1}{C} & -\frac{1}{CR} \end{bmatrix} \tag{7}$$

Filling phase

$$x(t)=\begin{bmatrix} v(t) \end{bmatrix},\quad b(t)=\begin{bmatrix} \frac{p_{LA}(t)}{R_{MV}} \end{bmatrix},\quad A(t)=\begin{bmatrix} -\frac{E(t,V(t))}{L_A} \end{bmatrix} \tag{8}$$

Parameters of SODEs for circulatory system with rotary blood pump

Isovolumic contraction/relaxation phase

$$x(t)=\begin{bmatrix} v(t) \\ i_A(t) \\ i_R(t) \\ p_A(t) \end{bmatrix},\quad b(t)=\begin{bmatrix} 0 \\ 0 \\ \frac{p_{BP}(t,i_R(t))}{L_P} \\ 0 \end{bmatrix},$$
$$A(t)=\begin{bmatrix} 0 & 0 & -1 & 0 \\ 0 & -\frac{r}{L_A} & 0 & 0 \\ \frac{E(t,V(t))}{L_P} & 0 & 0 & -\frac{1}{L_P} \\ 0 & \frac{1}{C} & \frac{1}{C} & -\frac{1}{CR} \end{bmatrix} \tag{9}$$

Ejection phase

$$x(t)=\begin{bmatrix} v(t) \\ i_A(t) \\ i_R(t) \\ p_A(t) \end{bmatrix},\quad b(t)=\begin{bmatrix} 0 \\ 0 \\ \frac{p_{BP}(t,i_R(t))}{L_P} \\ 0 \end{bmatrix},$$
$$A(t)=\begin{bmatrix} 0 & -1 & -1 & 0 \\ \frac{E(t,V(t))}{L_A} & -\frac{r}{L_A} & 0 & -\frac{1}{L_A} \\ \frac{E(t,V(t))}{L_P} & 0 & 0 & -\frac{1}{L_P} \\ 0 & \frac{1}{C} & \frac{1}{C} & -\frac{1}{CR} \end{bmatrix} \tag{10}$$

Filling phase

$$x(t)=\begin{bmatrix} v(t) \\ i_A(t) \\ i_R(t) \\ p_A(t) \end{bmatrix}, \quad b(t)=\begin{bmatrix} \frac{p_{LA}(t)}{R_{MV}} \\ 0 \\ \frac{p_{BP}(t,i_R(t))}{L_P} \\ 0 \end{bmatrix},$$

$$A(t)=\begin{bmatrix} -\frac{E(t,V(t))}{R_{MV}} & 0 & -1 & 0 \\ 0 & -\frac{r}{L_A} & 0 & 0 \\ \frac{E(t,V(t))}{L_P} & 0 & 0 & -\frac{1}{L_P} \\ 0 & \frac{1}{C} & \frac{1}{C} & -\frac{1}{CR} \end{bmatrix} \tag{11}$$

References

1. Umeki A, Nishimura T, Ando M, Takewa Y, Yamazaki K, Kyo S, Ono M, Tsukiya T, Mizuno T, Taenaka Y, Tatsumi E. Alteration of LV end-diastolic volume by controlling the power of the continuous-flow LVAD, so it is synchronized with cardiac beat: development of a native heart load control system (NHLCS). J Artif Organs. 2012;15:128–33.
2. Arakawa M, Nishimura T, Takewa Y, Umeki A, Ando M, Kishimoto Y, Fujii Y, Kyo S, Adachi H, Tatsumi E. Novel control system to prevent right ventricular failure induced by rotary blood pump. J Artif Organs. 2014;17:135–41.
3. Arakawa M, Nishimura T, Takewa Y, Umeki A, Ando M, Kishimoto Y, Kishimoto S, Fujii Y, Date K, Kyo S, Adachi H, Tatsumi E. Pulsatile support using a rotary left ventricular assist device with an electrocardiography-synchronized rotational speed control mode for tracking heart rate variability. J Artif Organs. 2016;19:204–7.
4. Date K, Nishimura T, Takewa Y, Kishimoto S, Arakawa M, Umeki A, Ando M, Mizuno T, Tsukiya T, Ono M, Tatsumi E. Shifting the pulsatility by increasing the change in rotational speed for a rotary LVAD using a native heart load control system. J Artif Organs. 2016;19:315–21.
5. Naito N, Nishimura T, Iizuka K, Takewa Y, Umeki A, Ando M, Ono M, Tatsumi E. Rotational speed modulation used with continuous-flow left ventricular assist device provides good pulsatility. Interact Cardiovasc Thorac Surg. 2018;26:119–23.
6. Pirbodaghi T, Weber A, Axiak S, Carrel T, Vandenberghe S. Asymmetric speed modulation of a rotary blood pump affects ventricular unloading. Eur J Cardiothorac Surg. 2013;43:383–8.
7. Vollkron M, Schima H, Huber L, Wieselthaler G. Interaction of the cardiovascular system with an implanted rotary assist device: simulation study with a refined computer model. Artif Organs. 2002;26:349–59.
8. Xu L, Fu M. Computer modeling of interactions of an electric motor, circulatory system, and rotary blood pump. ASAIO J. 2000;46:604–11.
9. Doshi D, Burkhoff D. Cardiovascular simulation of heart failure pathophysiology and therapeutics. J Cardiac Fail. 2016;22:303–11.
10. Wang Y, Loghmanpour N, Vandenberghe S, Ferreira A, Keller B, Gorcsan J, Antaki J. Simulation of dilated heart failure with continuous flow circulatory support. PLoS ONE. 2014;9:e85234.
11. Giridharan GA, Skliar M. Physiological control of blood pumps using intrinsic pump parameters: a computer simulation study. Artif Organs. 2006;30:301–7.
12. Wu Y. Adaptive physiological speed/flow control of rotary blood pumps in permanent implantation using intrinsic pump parameters. ASAIO J. 2009;55:335–9.
13. Vandenberghe S, Segers P, Meyns B, Verdonck P. Unloading effect of a rotary blood pump assessed by mathematical modeling. Artif Organs. 2003;27:1094–101.
14. Bozkurt S, Bozkurt S. In-silico evaluation of left ventricular unloading under varying speed continuous flow left ventricular assist device support. Biocybern Biomed Eng. 2017;37:373–87.
15. Htet ZL, Aye TP, Singhavilai T, Naiyanetr P. Hemodynamics during rotary blood pump support with speed synchronization in heart failure condition: a modelling study. Conf Proc IEEE Eng Med Biol Soc. 2015;2015:3307–10.
16. Guyton AC, Hall JE. Textbook of medical physiology. 11th ed. Philadelphia: Elsevier; 2005.
17. Zhong L, Ghista DN, Ng EY, Lim ST. Passive and active ventricular elastances of the left ventricle. Biomed Eng Online. 2005;4:10.
18. Moazami N, Fukamachi K, Kobayashi M, Smedira NG, Hoercher KJ, Massiello A, Lee S, Horvath DJ, Starling RC. Axial and centrifugal continuous-flow rotary pumps: a translation from pump mechanics to clinical practice. J Heart Lung Transplant. 2013;32:1–11.
19. Burkhoff D, Mirsky I, Suga H. Assessment of systolic and diastolic ventricular properties via pressure-volume analysis: a guide for clinical, translational and basic researchers. Am J Physiol Heart. 2005;289:501–12.
20. Soucy KG, Koenig SC, Giridharan GA, Sobieski MA, Slaughter MS. Defining pulsatility during continuous-flow ventricular assist device support. J Heart Lung Transplant. 2013;32:581–7.
21. Rich JD, Burkhoff D. HVAD flow waveform morphologies: theoretical foundation and implications for clinical practice. ASAIO J. 2017;63:526–35.
22. Vandenberghe S, Segers P, Antaki JF, Meyns B, Verdonck PR. Hemodynamic modes of ventricular assist with a rotary blood pump: continuous, pulsatile, and failure. ASAIO J. 2005;51:711–8.
23. Yamazaki K, Saito S, Kihara S, Tagusari O, Kurosawa H. Completely pulsatile high flow circulatory support with a constant-speed centrifugal blood pump: mechanisms and early clinical observations. Gen Thorac Cardiovasc Surg. 2007;55:158–62.
24. Imamura T, Kinugawa K, Nitta D, Hatano M, Kinoshita O, Nawata K, Ono M. Advantage of pulsatility in left ventricular reverse remodeling and aortic insufficiency prevention during left ventricular assist device treatment. Circ J. 2015;79:1994–9.
25. Hatano M, Kinugawa K, Shiga T, Kato N, Endo M, Hisagi M, Nishimura T, Yao A, Hirata Y, Kyo S, Ono M, Nagai R. Less frequent opening of the aortic valve and a continuous flow pump are risk factors for postoperative onset of aortic insufficiency in patients with a left ventricular assist device. Circ J. 2011;75:1147–55.
26. Rose AG, Park SJ, Bank AJ, Miller LW. Partial aortic valve fusion induced by left ventricular assist device. Ann Thorac Surg. 2000;70:1270–4.
27. Moazami N, Dembitsky WP, Adamson R, Steffen RJ, Soltesz EG, Starling RC, Fukamachi K. Does pulsatility matter in the era of continuous-flow blood pumps? J Heart Lung Transplant. 2015;34:999–1004.
28. Saito T, Wassilew K, Gorodetski B, Stein J, Falk V, Krabatsch T, Potapov E. Aortic valve pathology in patients supported by continuous-flow left ventricular assist device. Circ J. 2016;80:1371–7.
29. Tolpen S, Janmaat J, Reider C, Kallel F, Farrar D, May-Newman K. Programmed speed reduction enables aortic valve opening and increased pulsatility in the LVAD-assisted heart. ASAIO J. 2015;61:540–7.
30. Bazan O, Ortiz JP. Duration of systole and diastole for hydrodynamic testing of prosthetic heart valves: comparison between ISO 5840 standards and in vivo studies. Braz J Cardiovasc Surg. 2016;31:171–3.

31. Ising M, Warren S, Sobieski MA, Slaughter MS, Koenig SC, Giridharan GA. Flow modulation algorithms for continuous flow left ventricular assist devices to increase vascular pulsatility: a computer simulation study. Cardiovasc Eng Technol. 2011;2:90–100.
32. Bozkurt S, van de Vosse FN, Rutten MC. Enhancement of arterial pressure pulsatility by controlling continuous-flow left ventricular assist device flow rate in mock circulatory system. J Med Biol Eng. 2016;36:308–15.
33. Ising MS, Sobieski MA, Slaughter MS, Koenig SC, Giridharan GA. Feasibility of pump speed modulation for restoring vascular pulsatility with rotary blood pumps. ASAIO J. 2015;61:526–32.

Publisher's Note Springer Nature remains neutral with regard to jurisdictional claims in published maps and institutional affiliations.